

Excitation of fullerene ions during grazing scattering from a metal surface

S. Wethekam* and H. Winter

Institut für Physik, Humboldt-Universität zu Berlin, Brook-Taylor-Strasse 6, D-12489 Berlin, Germany

(Received 2 March 2007; revised manuscript received 16 July 2007; published 12 September 2007)

Angular distributions, fragmentation, and charge fractions are studied for grazing scattering of C_{60}^+ fullerenes with keV energies from a clean and flat Al(001) surface. At low energies for the motion along the surface normal, C_{60}^+ ions are scattered nearly elastically, whereas for larger normal energies energy loss is substantial. We compare our experimental results with classical trajectory simulations exploiting the Tersoff potential between atoms in the cluster and different types of interaction potentials for the cluster with the surface. The internal energy of scattered clusters is deduced from the analysis of fragments. We observe that the loss of kinetic energy for the motion along the surface normal is transferred to internal excitations of the cluster, whereas the energy transfer to the metal surface is negligible. The charge state distributions for scattered projectiles can be understood by a full neutralization of incident ions at the surface and subsequent delayed electron emission.

DOI: [10.1103/PhysRevA.76.032901](https://doi.org/10.1103/PhysRevA.76.032901)

PACS number(s): 79.20.Rf, 79.60.Bm, 78.30.Na

I. INTRODUCTION

Studies on the interaction of hyperthermal molecular species scattered from solid surfaces are of interest from a fundamental point of view and for technological applications, as, e.g., catalysis, particle detectors, etc. However, compared to the large body of literature and considerable progress toward a quantitative understanding of atom-surface interactions in the last decades [1,2], studies on the interactions of molecules and clusters with surfaces are rare and suffer from an enhanced complexity introduced by the additional degrees of freedom. During collisions, internal excitations of the molecules can trigger delayed processes, such as electron emission or fragmentation, which may dominate the outcome of experiments [3]. Due to their symmetrical shape, stability, well-known electronic structure, and simple production fullerene ions, especially C_{60}^+ , are promising candidates for exploring cluster-surface interactions.

From the few studies on the impact of C_{60} ions on surfaces [3], we mention work by Lill *et al.* [4], where 100–700 eV C_{60}^+ ions are scattered under near-normal incidence from graphite, diamond, WSe, and oxidized Ni surfaces. The scattering process with the surface was observed to be inelastic with energies of only 3–11 eV for outgoing clusters. From the analysis of fragment spectra it was concluded that 15%–40% of the incident energy was converted into internal excitation of the clusters. For impact on fullerite surfaces rainbow scattering was observed. Beck *et al.* [5] have scattered C_{60}^+ and other fullerenes with energies of several 100 eV from clean and adsorbate covered graphite surfaces under an angle of incidence of 45°. They found energies for outgoing clusters of about 20 eV independent of the incident energy. From fragment spectra it was concluded that in case of a clean graphite surface about 30% of the collision energy (10% for the adsorbate covered surface) was transferred to internal excitations. For collision energies larger than about

400 eV the clusters were shattered upon surface impact. In order to reduce the energy transfer to the surface Hillenkamp *et al.* [6] performed measurements at a near-grazing angle of incidence of 15°. However, a considerable fraction of the projectile energy was still transferred to the crystal lattice of the surface. Charge state distributions revealed that C_{60}^+ was efficiently neutralized (>99% of scattered clusters were neutral), whereas the fraction of negative ions amounts to some 10^{-3} for a graphite surface [7]. Kolodney *et al.* [8] have scattered neutral C_{60} molecules with energies of some 10 eV from a polycrystalline nickel surface and studied carbon deposition on the surface. Furthermore, angular and energy distributions as well as the vibrational excitation of scattered clusters were investigated. The energy of scattered projectiles scaled linearly with the impact energy, and kinetic energy losses of 40%–85% (depending on the scattering angle) were found. The internal excitation of the fullerenes was below 2% of the impact energy, which is much lower than observed in other experiments with fullerenes. From shifts of the angular distributions caused by the attractive force owing to image charge interaction [9] for negative C_{60}^- and neutral C_{60}^0 clusters formed during near-grazing scattering from a carbonized nickel surface, a distance for the formation of negative ions of about 13 Å was derived [10]. This value is in accord with the distance for negative ion formation derived from negative ion yields measured for near-normal incidence [11]. Recently, Kaplan *et al.* [12] investigated a post-collision shattering of C_{60}^- during near-grazing scattering from a gold surface with energies of several 100 eV. For potential electron emission during neutralization of multi-charged fullerenes at a gold surface no dependence on the cluster's charge was found [13]. This was interpreted in terms of a fast quenching of the primary excitation energy via fragmentation of the projectiles.

Cluster-surface scattering experiments performed at a grazing angle of incidence of about 1°, i.e., surface channeling conditions [14], have been reported recently by Tamehiro *et al.* [15]. For 3 keV C_{60}^+ ions and C_{60}^0 atoms scattered from a KCl(001) surface, clusters were elastically reflected for normal energies up to about 20 eV with negligible energy

*Author to whom correspondence should be addressed; stephan.wethekam@physik.hu-berlin.de

transfer to the target surface. The neutralization rate for positive clusters as a function of distance from the surface was derived by measuring fractions of surviving ions as a function of the polar and azimuthal angle of incidence.

We have recently scattered C_{60}^+ ions with keV energies under a grazing angle of incidence of about 1° from an Al(001) surface. From the analysis of angular distributions as a function of azimuthal rotation close to a low-indexed direction we found that crystal channels formed by strings of atoms in the surface plane can induce a rotation of the cluster that results in an azimuthal deflection and guiding of clusters along low-indexed directions [16]. The neutralization of C_{60}^+ and C_{60}^{2+} ions at Al(001) was studied via shifts of angular distributions due to image charge attraction prior to neutralization [9,17]. The observed shifts were in good accord with calculations using a classical over-the-barrier charge transfer model in which the fullerene was modeled as a polarizable sphere [18]. It was concluded that final neutralization occurs at a distance of $6.6a_0$ (fullerene cage radius $6.7a_0$) between the closest C atom in the fullerene and the surface [17].

In this work, we measured angular and charge state distributions as well as fragmentation of scattered clusters for C_{60}^+ ions scattered with keV energies under a grazing angle of incidence of typically 1° from an Al(001) surface. Scattering proceeds in the regime of surface channeling in a series of small-angle scattering events with surface atoms, where the motions of projectiles parallel and normal with respect to the surface are widely decoupled [2,14]. Within the resolution of our experiments, we observe no dependence of our data on the grazing angle of incidence for constant normal energy. The trajectory length determines the energy transfer to the surface and depends on the grazing angle of incidence. Therefore, the observation that our data does not show a dependence on angle for constant normal energy is consistent with a negligible energy transfer to the surface [2]. For normal energies smaller than about 5–7 eV the clusters are scattered elastically, while for normal energies larger than about 10 eV scattering is inelastic and normal energy losses can amount to more than 90% of the incident normal energy. The data is compared to trajectory calculations exploiting the empirical Tersoff potential [19] for the cluster and different interaction potentials for the cluster with the surface. By an analysis of fragment spectra of scattered clusters we investigate the transfer of energy to internal degrees of freedom of the clusters. Delayed electron emission is studied via charge fractions of scattered clusters.

II. EXPERIMENT AND RESULTS

In our experiments we have scattered 2.5–62.5 keV C_{60}^+ ions under grazing angles of incidence ranging from 0.8° to 3.1° along high-indexed (“random”) directions from a clean and atomically flat Al(001) surface. The target was prepared by cycles of grazing sputtering with 25 keV Ar^+ ions and subsequent annealing at $500^\circ C$ for about 10 min. The quality of the surface was controlled by the shape of angular distributions [2]. C_{60}^+ ions were produced by evaporation of C_{60} powder in a 10 GHz electron cyclotron resonance (ECR) ion source (Nanogan, Pantechique) at an Ar pressure of

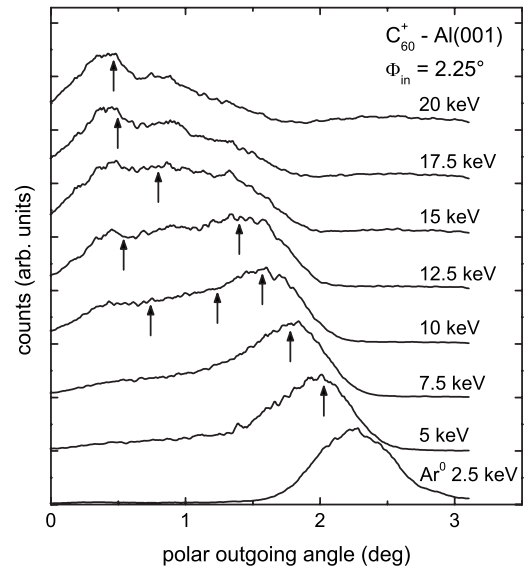


FIG. 1. Waterfall plot of polar angular distributions for scattering of Ar^0 atoms and C_{60}^+ clusters with energies indicated under a grazing angle of incidence of 2.25° from Al(001). Ticks on the vertical axis indicate offsets of zero level for distributions. Arrows indicate outgoing angles for which fragment distributions have been measured (see below).

10^{-4} mbar [15,20,21]. Ions from the source are mass separated by means of a magnet. The clusters have a relatively high internal excitation energy of about 35 eV (see below) so that already a small additional energy transfer to internal excitations during the collision with the surface triggers delayed fragmentation. Trajectories of scattered clusters are hardly affected by internal excitations of the incoming clusters [5] (see also simulations below). Angular distributions for scattered particles are measured with a position-sensitive micro-channel-plate detector (Roentdek, Kelkheim-Ruppertshain) at a distance of 66 cm behind the target. Spatial variations of the detection efficiency of the channel plate were corrected by wobbling the direct beam over the active area of the detector. As reference for the angle of incidence serves scattering of Ar^0 atoms, which are elastically reflected from the surface [2]. Projectiles were dispersed with respect to their charge and fragment state in an electric field between target and detector.

A. Inelastic scattering, analysis of angular distributions

In Fig. 1 we show polar angular distributions after scattering of $E_0=5-20$ keV C_{60}^+ ions as well as 2.5 keV Ar^0 atoms from the Al(001) surface under a grazing angle of incidence of $\Phi_{in}=2.25^\circ$. For low energies the clusters are scattered nearly elastically with well-defined peaked angular distributions similar to the distribution for Ar^0 atoms. For increased energies, the clusters are scattered subsonically, the distributions become broader, and deviate from a Gaussian line shape. In Fig. 2 we show the outgoing normal energy $E_z^{out}=E_0 \sin^2 \Phi_{out}$ as a function of incoming normal energy $E_z^{in}=E_0 \sin^2 \Phi_{in}$ obtained from the peak positions (full symbols) as well as the positions of both half-maxima (open

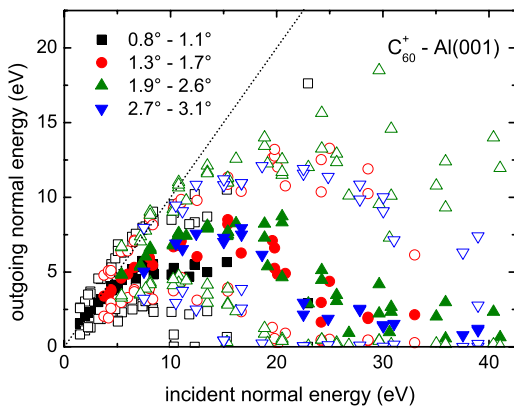


FIG. 2. (Color online) Outgoing normal energy E_z^{out} as a function of incident normal energy E_z^{in} for clusters scattered under angles of incidence indicated. Full symbols (open symbols): results obtained from peak (half-maximum) positions of angular distributions. The dotted curve indicates specular reflection.

symbols) of angular distributions for different angles of incidence. For low normal energies $E_z^{\text{in}} \leq 5-7$ eV the clusters are scattered almost elastically while for normal energies $E_z^{\text{in}} \geq 10$ eV the outgoing normal energy is substantially reduced, $E_z^{\text{out}} \ll E_z^{\text{in}}$. For normal energies $E_z^{\text{in}} \geq 30$ eV the majority of scattered clusters leaves the surface with normal energies $E_z^{\text{out}} \leq 5$ eV, which is equivalent to a normal energy loss of about 90%. Within our experimental resolution, the data is independent of the angle of incidence (trajectory length, number of small-angle collisions with surface atoms) for constant normal energy. From this finding we conclude that the observed energy loss cannot be attributed to an energy transfer to the surface.

In order to analyze the angular distributions we performed classical trajectory calculations using the empirical Tersoff potential [19] for the C-C interaction. The Tersoff potential contains both two-body and three-body contributions that depend on the local environment of the atoms (bond angles and bond order). It was optimized to describe structural and energetic properties of a number of carbon structures. Before the collision with the surface, the clusters were relaxed to equilibrium, consistent with the Tersoff potential. This resulted in small changes of the atom positions [22] only. For each trajectory the clusters were randomly oriented and placed with respect to a unit cell of the surface. The Al(001) surface was represented by a rigid cluster of $7 \times 7 \times 2$ atoms centered below the projectile and Newton equations of motion were numerically solved using a fourth-order Runge-Kutta method [23]. Correlated thermal vibrations of target atoms were included within the Debye model at $T=300$ K and Debye temperatures from Ref. [24]. For details see Ref. [25]. Temperature effects have only a minor effect on the results presented here. Our simulations have been successfully applied to the description of azimuthal shifts of angular distributions, observed for grazing scattering in the vicinity of low-indexed directions of an Al(001) surface [16]. Also, the onset of shattering of C_{60} clusters during impact on a hard wall at much larger energies than in our experiments analyzed using the Tersoff potential by Sabin *et al.* [26] is in

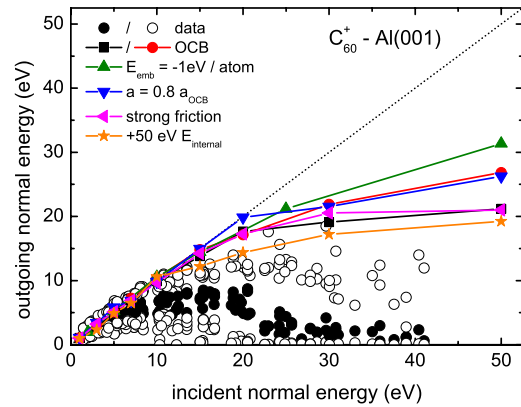


FIG. 3. (Color online) Comparison of data of Fig. 2 (circles) for outgoing normal energy E_z^{out} as a function of incident normal energy E_z^{in} for grazing scattering of C_{60}^+ from Al(001) to results from simulations (curves with symbols). The dotted curve indicates specular reflection. For details see the text.

quantitative accord with our simulations. As the interaction potential of the clusters with the surface is only vaguely known, we have implemented different types of interaction potentials.

In Fig. 3 we compare results from our trajectory calculations (curves with symbols) with the data of Fig. 2 (circles). Fifteen to twenty trajectories have been calculated for each point and the outgoing normal energy E_z^{out} has been derived from the mean outgoing angle $\langle \Phi_{\text{out}} \rangle$ via $E_z^{\text{out}} = E_0 \sin^2 \langle \Phi_{\text{out}} \rangle$, where E_0 denotes the projectile energy. The accuracy of the calculations is limited by the number of calculated trajectories. In order to estimate the uncertainty due to this statistical effect we have included two curves calculated using a Moliere potential with a corrected Firsov screening length a_{OCB} by O'Connor and Biersack (OCB) [27] for the interaction of the cluster atoms with the surface. In addition, we present results obtained for a planar attractive potential for embedding carbon atoms into the electron gas in front of the surface (added to the OCB potential) via $E_c(z) = -1 \text{ eV} [1 - \tanh(z/a_0 - 4)]/2$, which vanishes for larger distances z and saturates at an energy $E_{\text{emb}} = -1$ eV inside the crystal. This potential reproduces the data reported in [16] and typical adsorption energies for molecules at metal surfaces of a few eV [28]. Furthermore, we show results for a reduced screening length $a = 0.8 a_{\text{OCB}}$, i.e., a relatively hard surface. In order to check a possible influence of electronic friction on our results we performed calculations using a friction force for carbon atoms in a jellium metal [2,29] extrapolated to the velocities v relevant here assuming proportionality to v . The distance dependence of the friction force was derived from the electron density [30] for a jellium edge at $z = 1.91 a_0$. This friction force per carbon atom was further increased by almost an order of magnitude resulting in an estimate on an upper bound for the cluster-surface friction force. In addition, we present calculations for incident clusters with an internal excitation of 50 eV distributed over the vibrational degrees of freedom.

The results in Fig. 3 reveal that the outgoing normal energy does only slightly depend on the choice of the cluster-

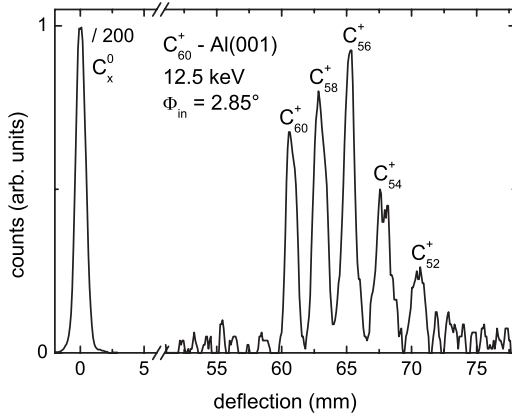


FIG. 4. Fragment-size distribution for scattering of 12.5 keV C_{60}^+ clusters under $\Phi_{in}=2.85^\circ$ from Al(001). Signal for neutral clusters C_x^0 scaled down by factor 200.

surface potential, the electronic friction force, or the excitation of incident clusters. In the simulations, the clusters have significantly larger outgoing normal energies than found in our experiments. The discrepancies of the simulations with the data will most likely stem from deficiencies in the description of the binding of the deformed cluster by the Tersoff potential. A further analysis using more sophisticated carbon potentials [3,31,32] and a realistic modeling of the cluster-surface interaction, however, goes beyond the scope of the present paper.

Our data is different than the results of Kimura *et al.* [15] for grazing scattering of C_{60}^+ from KCl(001), where elastic scattering for larger normal energies up to 20 eV was found. Preliminary measurements performed by us with a LiF(001) surface show similar results as reported for KCl. In the case of KCl(001) and LiF(001), C_{60}^+ clusters are predominantly scattered as positive ions while in case of the metal surface Al(001) they are efficiently neutralized (cf. Fig. 7). The differences have to be attributed to different elastic properties of neutral and charged C_{60} or different interactions with the metal and insulator surfaces. We note that our results cannot be compared with former studies performed at larger angles of incidence [4,5,8] (see above), where the surface is strongly deformed upon cluster impact.

B. Internal excitation, fragmentation and delayed electron emission

In order to analyze the internal excitation of scattered clusters we have measured fragment distributions for scattered projectiles at the maxima and also at other positions of the angular distributions (e.g., arrows in Fig. 1). A small slit was placed within the angular distribution and charged fragments were dispersed in an electric field. As an example, we show a fragment size distribution for scattering of 12.5 keV C_{60}^+ clusters under $\Phi_{in}=2.85^\circ$ in Fig. 4. Charged C_x^+ fragments are well identified in the spectra. In our experiment only even-numbered C_x^+ fragments were found, which indicates that the fragment spectra result from delayed evaporation of C_2 segments and delayed electron emission [3]. Shat-

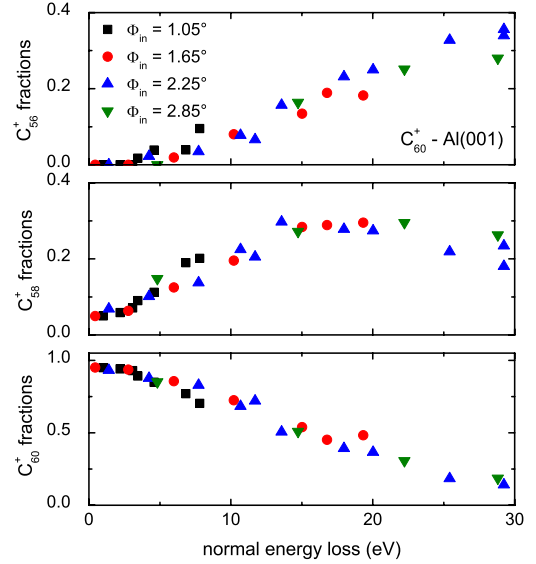


FIG. 5. (Color online) C_{60}^+ , C_{58}^+ , and C_{56}^+ fragment fractions normalized to $C_{60}^+ - C_{52}^+$ as a function of normal energy loss ΔE_z for different angles of incidence indicated.

tering at the surface results in both even and small odd fragments and is expected only for much larger normal energies ≥ 200 eV [4,5,8,12,26]. At the onset of shattering the distribution of large fragments is centered at about C_{50}^+ [5], which indicates that larger internal excitations of the clusters than found in our experiments (see below) are needed to induce shattering of the clusters at the surface. When plotted as a function of the normal energy loss $\Delta E_z = E_z^{in} - E_z^{out}$ the fragment distributions measured at different positions of the angular distributions fell on common curves. In Fig. 5 we show normalized fractions of C_{60}^+ , C_{58}^+ , and C_{56}^+ ions as a function of normal energy loss ΔE_z for different angles of incidence. For a given E_z the data does not depend on the angle of incidence so that an energy transfer to the surface can be neglected. In Fig. 6 we present fragment fractions of $C_{60}^+ - C_{52}^+$ as a function of normal energy loss ΔE_z . For low normal energies and normal energy losses predominantly intact clusters are found, but as the normal energy loss is increased fragmentation sets in, the C_{60}^+ fractions decrease, and smaller fragments appear in the spectrum.

In order to estimate the internal energy E_{in} of the scattered clusters, we performed simulations of fragment spectra using an Arrhenius representation of rate constants for delayed C_2 loss and electron emission. Based on the concept of the microcanonical temperature [33–36] we describe relative populations $F_m^q(t)$ of C_{60-2m}^{q+} fragments with charge $q+$ that have emitted m C_2 fragments by the rate equation

$$\begin{aligned} \frac{dF_m^q(t)}{dt} = & -F_m^q(t)(k_{m \rightarrow m+1}^q + k_m^{q \rightarrow q+1}) + F_{m-1}^{q-1}(t)k_m^{q-1 \rightarrow q} \\ & + F_{m-1}^q(t)k_{m-1 \rightarrow m}^q, \end{aligned} \quad (1)$$

where

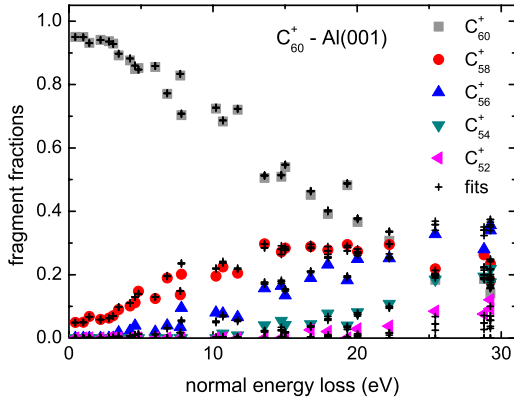


FIG. 6. (Color online) $C_{60}^+ - C_{52}^+$ fragment fractions as a function of normal energy loss ΔE_z (symbols). Plus signs show results from fits of fragment spectra. For details see the text.

$$k_{m \rightarrow m+1}^q = A_d \exp\left(-\frac{E_d}{k_B T_e}\right), \quad (2)$$

$$k_m^{q \rightarrow q+1} = A_{\text{ion}}(T_f) \exp\left(-\frac{E_{\text{ion}}}{k_B T_e}\right) \quad (3)$$

are Arrhenius representations of the delayed evaporation rates and the ionization rates, respectively. E_d is the dissociation energy for C_2 loss, E_{ion} the $(q+1)$ th ionization energy, and T_e (T_f) the emission (fragment) temperatures of the cluster, which are related to the microcanonical temperature T_m of the cluster via

$$T_e = T_m - \frac{E_{d\text{ion}}}{2c_m}, \quad (4)$$

$$T_f = T_m - \frac{E_{d\text{ion}}}{c_m}, \quad (5)$$

where the second term in Eq. (4) represents the finite-heat-bath correction [33,37] and c_m is the microcanonical heat capacity. The caloric curve for C_{60} can be calculated using harmonic oscillator partition functions [38] and is well approximated for parameters relevant here by [38,39]

$$E_{\text{in}} = 0.0147 \frac{\text{eV}}{\text{K}} T_m - 8.46 \text{ eV}, \quad (6)$$

with a heat capacity only slightly different from high-temperature limit $(3 \cdot 60 - 7)k_B = 0.0149 \frac{\text{eV}}{\text{K}}$. Therefore, we approximate the microcanonical heat capacity by

$$c_m = \frac{3n-7}{173} 0.0147 \frac{\text{eV}}{\text{K}}, \quad (7)$$

where $n=60-2m$ is the number of atoms in the cluster. For the Arrhenius factors A_d [36,40,41] and A_{ion} [35,39], the dissociation energies E_d [36,40,41], and the ionization energies [42–44] we use the values of Concina *et al.* [45,46], which are given in Table I. The Arrhenius A factors and dissociation energies are not precisely known, but the results for the internal energies are not sensitive to their exact choice. In the

TABLE I. Parameters used in the simulation of the chain of ionization and C_2 emission [42–46]. Parameters for ionization of charged fullerenes are not relevant for the analysis here as they predominantly decay by dissociation. For details see the text.

	E_d (eV)	A_d (s ⁻¹)	E_{ion} (eV)	$A_{\text{ion}}(T_f)$ (s ⁻¹)
C_{60}^0	10.6	2.3×10^{21}	7.6	$1 \times 10^{15} \frac{T_f}{4000 \text{ K}}$
C_{58}^0	8.4			
C_{56}^0	8.6	2×10^{19}	7.1	$5 \times 10^{14} \frac{T_f}{4000 \text{ K}}$
C_{54}^0	8.4			
C_{52}^0	8.4			
C_{60}^+	10.1	1.2×10^{21}	11.4	$5 \times 10^{14} \frac{T_f}{4000 \text{ K}}$
C_{58}^+	8.4			
C_{56}^+	8.6	2×10^{19}	11.4	$5 \times 10^{14} \frac{T_f}{4000 \text{ K}}$
C_{54}^+	8.4			
C_{52}^+	8.4			

calculations we start with neutral C_{60}^0 with an internal energy E_{in} and solve the differential equations (1) up to the time (\sim few μs) when the projectiles pass the electric field plates at a distance of 30 cm behind the target. Then the charge fractions as well as the fractions of singly charged fragments are extracted for comparison with data.

The internal energies of the scattered clusters were derived by fitting the fragment spectra with Gaussian distributions of internal energies. The mean internal energy and the width of the energy distribution can be unequivocally derived only for fragment spectra with at least three fragments present, which is the case for normal energy losses $\Delta E_z > 13$ eV. We have first analyzed data in this region and found a linear dependence $\text{FWHM} = 0.47\Delta E_z + 14$ eV of the width of the energy distribution as a function of the normal energy loss ΔE_z (cf. dashed curve in Fig. 8). This function was extrapolated to $\Delta E_z < 13$ eV and used to fix the width in the low energy region where only the mean internal energy was derived from fits of the fragment spectra. As shown in Fig. 6 our fits (plus signs) reproduce the measured spectra (symbols).

In Fig. 7 we show positive ion fractions for large fragments (full circles) as a function of normal energy after scattering of C_{60}^+ ions from Al(001). Ion fractions are small and consistent with an efficient neutralization of clusters on the incoming part of the trajectory [17]. Those fractions can be calculated from the internal energies (cf. Fig. 8) derived from the fits of the fragment spectra under the assumption that the clusters are efficiently neutralized at the surface and that ions predominantly result from delayed electron emission as described by Eq. (1). For A_d and A_{ion} as given in Table I, the calculated ion fractions are a factor three too small (squares in Fig. 7). The agreement with measured ion fractions is improved for increased A_{ion} or reduced A_d leading to enhanced probabilities for delayed electron emission events.

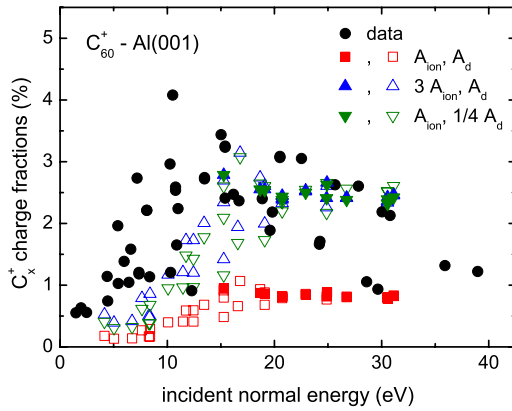


FIG. 7. (Color online) Measured fractions of positive ions after scattering of C_{60}^+ ions from Al(001) (full circles) as a function of incident normal energy E_z^{in} . Data compared to charge fractions derived from fits of fragment spectra using different rate prefactors as indicated. Full symbols: results from fits of both mean value and FWHM of internal energy distribution. Open symbols: results from fits of mean energy only, with FWHM from linear approximation. For details see the text and Fig. 8.

Compared to the uncertainties for the knowledge of the (temperature-dependent) Arrhenius A factors and dissociation energies [3,33–36,39–41,45–47] only moderate adjustments of the rate constants are needed and simulations using $(3A_{\text{ion}}; A_d)$ (upward triangles) or $(A_{\text{ion}}; \frac{1}{4}A_d)$ (downward triangles) are in better accord with the data. The open (full) symbols show results where the linear extrapolation for the width of the energy distribution was used (not used).

In Fig. 8 we present mean internal energies E_{in} and FWHMs of the Gaussian energy distributions as a function of the normal energy loss ΔE_z as deduced from fits of the fragment distributions using different Arrhenius A factors. The A factors have only a minor effect on the internal energy

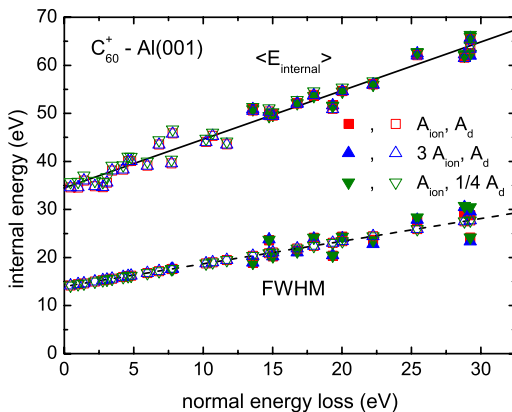


FIG. 8. (Color online) Mean internal energy E_{in} and FWHM of internal energy distribution derived from fits of fragment spectra as a function of normal energy loss ΔE_z for different rate prefactors indicated. Full symbols: results from fits of both mean value and FWHM of internal energy distribution. Open symbols: results from fits of mean energy only, with FWHM from linear approximation $\text{FWHM} = 0.47\Delta E_z + 14$ eV. The solid line corresponds to $E_{\text{in}} = \Delta E_z + 34.5$ eV, which means full transfer of normal energy loss to internal excitations of clusters. For details see the text.

distributions. The mean internal energies and the FWHM of the energy distributions for the scattered clusters increase with increasing normal energy loss. The solid line representing $E_{\text{in}} = \Delta E_z + 34.5$ eV is in good accord with our analysis and corresponds to a full transfer of normal energy loss to internal excitations. Then the initial internal energy for incoming clusters is about 35 eV.

The efficiency for energy transfer to internal excitations is larger than found in previous studies [4,5,8], because the incoming energy is not transferred to the surface. We note that our results measured for a range of grazing angles of incidence of $\Phi_{\text{in}} = 1^\circ - 3^\circ$ scale with the normal energy loss, but do not depend on the motion parallel to the surface. From our trajectory simulations using typical electronic friction forces for atoms [2,29] one would expect excitations of clusters from several up to some 10 eV. Keeping the normal energy fixed, the energy loss due to electronic friction $\int dE/dx dx$ is expected to scale as $1/\sin^2 \Phi_{\text{in}}$, since both the trajectory length as well as the stopping power dE/dx scale as $1/\sin \Phi_{\text{in}}$ and $dE/dx \propto v = v_z/\sin \Phi_{\text{in}}$ in the regime of slow atom- (molecule-) surface collisions. The distance of closest approach is the same for the same normal energies. This would result in a factor of 3 difference for the parallel energy loss for $\Phi_{\text{in}} = 1.65^\circ$ and $\Phi_{\text{in}} = 2.85^\circ$. The internal energies determined from the fragment spectra for both angles of incidence, however, are the same within the experimental uncertainty. Possible explanations could be small electronic stopping forces for C_{60}^+ in front of the metal surface or that the energy of an additional rotational excitation of the cluster as a whole induced by friction parallel to the surface does not affect delayed fragmentation. Therefore, it is of interest to determine also the energy loss of the complete projectile motion by time-of-flight techniques in future experiments.

III. SUMMARY AND CONCLUSIONS

We have scattered keV C_{60}^+ fullerenes from a clean and flat Al(001) surface under grazing angles of incidence of typically 1° along high-indexed (“random”) directions and recorded angular, fragment, and charge state distributions for scattered projectiles. The results show no dependence on the grazing angle of incidence (trajectory length) for constant energy of motion of projectiles along the surface normal. This shows that energy transfer to the surface and effects of the parallel motion on the data are negligible. For normal energies $E_z \leq 5-7$ eV the projectiles are scattered nearly elastically, but for higher normal energies projectiles lose a substantial amount of their normal energy. We compare angular distributions with results from trajectory simulations using the empirical Tersoff potential for the C-C interactions with the surface. The agreement with the data is poor and more sophisticated theoretical attempts are needed to describe angular distributions. As the energy transfer to the surface is negligible for our scattering conditions, the normal energy loss is expected to be transferred to internal excitations of scattered fullerenes. The internal energy of the scattered clusters was deduced from fitting fragment distributions using an Arrhenius ansatz for the rate constants for delayed C_2 loss

and delayed electron emission. From our data we conclude that the impinging clusters have excitation energies of about 35 eV. These energies are sufficiently large in order to study small energy transfers to internal degrees of freedom via the analysis of fragments. Charge state distributions for scattered projectiles are consistent with a full neutralization of incident ions at the surface and subsequent delayed electron emission. The normal energy loss is completely transferred to internal excitations of the cluster, whereas excitations due to the parallel motion are negligible. The efficiency for the transfer of normal energy to internal excitations of the clusters of up to 90% is much higher than found in previous studies on

fullerene-surface collisions. Finally, we point out that studies as performed here provide an interesting regime of collisions of clusters with a hard wall, since the energy transfer to the surface turns out to be negligible. This might offer an unique testing ground for the description of C_{60} potentials.

We thank the DFG (Project No. Wi 1336) for financial support and K. Maass and A. Schüller for their assistance in the preparation and running of the experiments. Discussions with Professor K. Kimura (Kyoto, Japan), Professor H. Cederquist (Stockholm, Schweden), and Professor E.E.B. Campbell (Göteborg, Schweden) are gratefully acknowledged.

- [1] J. Los and J. J. C. Geerlings, *Phys. Rep.* **190**, 133 (1990).
 [2] H. Winter, *Phys. Rep.* **367**, 387 (2002).
 [3] E. E. B. Campbell and F. Rohmund, *Rep. Prog. Phys.* **63**, 1061 (2000); E. E. B. Campbell, *Fullerene Collision Reactions* (Kluwer Academic, London, 2003).
 [4] Th. Lill, H.-G. Busmann, F. Lacher, and I. V. Hertel, *Chem. Phys.* **193**, 199 (1995).
 [5] R. D. Beck, J. Rockenberger, P. Weiss, and M. M. Kappes, *J. Chem. Phys.* **104**, 3638 (1996).
 [6] M. Hillenkamp, J. Pfister, M. M. Kappes, and R. P. Webb, *J. Chem. Phys.* **111**, 10303 (1999).
 [7] M. Hillenkamp, J. Pfister, and M. M. Kappes, *J. Chem. Phys.* **114**, 10457 (2001).
 [8] E. Kolodney, B. Tspinyuk, A. Bekkerman, and A. Budrevich, *Nucl. Instrum. Methods Phys. Res. B* **125**, 170 (1997).
 [9] H. Winter, *J. Phys.: Condens. Matter* **8**, 10149 (1996).
 [10] A. Bekkerman, B. Tspinyuk, S. Verkhoturov, and E. Kolodney, *J. Chem. Phys.* **109**, 8652 (1998).
 [11] A. Bekkerman, B. Tspinyuk, and E. Kolodney, *Phys. Rev. B* **61**, 10463 (2000).
 [12] A. Kaplan, A. Bekkerman, E. Gordon, B. Tspinyuk, M. Fleischer, and E. Kolodney, *Nucl. Instrum. Methods Phys. Res. B* **232**, 184 (2005).
 [13] H. P. Winter, M. Vana, G. Betz, F. Aumayr, H. Drexel, P. Scheier, and T. D. Märk, *Phys. Rev. A* **56**, 3007 (1997).
 [14] D. Gemmell, *Rev. Mod. Phys.* **46**, 129 (1974).
 [15] S. Tamehiro, T. Matsushita, K. Nakajima, M. Suzuki, and K. Kimura, *Nucl. Instrum. Methods Phys. Res. B* **256**, 16 (2007).
 [16] S. Wethekam, A. Schüller, and H. Winter, *Nucl. Instrum. Methods Phys. Res. B* **258**, 68 (2007).
 [17] S. Wethekam, H. Winter, H. Cederquist, and H. Zettergren, *Phys. Rev. Lett.* **99**, 037601 (2007).
 [18] H. Zettergren, H. T. Schmidt, H. Cederquist, J. Jensen, S. Tomita, P. Hvelplund, H. Lebius, and B. A. Huber, *Phys. Rev. A* **66**, 032710 (2002).
 [19] J. Tersoff, *Phys. Rev. Lett.* **61**, 2879 (1988).
 [20] R. Völpel, G. Hofmann, M. Steidl, M. Stenke, M. Schlapp, R. Trassl, and E. Salzborn, *Phys. Rev. Lett.* **71**, 3439 (1993).
 [21] S. Biri, A. Valek, L. Kenéz, A. Jánossy, and A. Kitagawa, *Rev. Sci. Instrum.* **73**, 881 (2002).
 [22] www.ccl.net/cca/data/fullerenes/
 [23] W. H. Press, S. A. Teukolsky, W. T. Vetterling, and B. P. Flannery, *Numerical Recipes in C++* (Cambridge University Press, Cambridge, 2002).
 [24] D. P. Jackson, *Surf. Sci.* **43**, 431 (1974).
 [25] S. Wethekam and H. Winter, *Nucl. Instrum. Methods Phys. Res. B* **258**, 48 (2007).
 [26] R. T. Chancey, L. Oddershede, F. E. Harris, and J. R. Sabin, *Phys. Rev. A* **67**, 043203 (2003).
 [27] D. J. O'Connor and J. P. Biersack, *Nucl. Instrum. Methods Phys. Res. B* **15**, 14 (1986).
 [28] M. J. Puska and R. M. Nieminen, *Phys. Rev. B* **43**, 12221 (1991).
 [29] M. Alducin, A. Arnau, and I. Nagy, *Phys. Rev. A* **68**, 014701 (2003).
 [30] J. R. Smith, *Phys. Rev.* **181**, 522 (1969).
 [31] D. W. Brenner, *Phys. Rev. B* **42**, 9458 (1990).
 [32] D. W. Brenner, O. A. Shenderova, J. A. Harrison, S. J. Stuart, B. Ni, and S. B. Sinnott, *J. Phys.: Condens. Matter* **14**, 783 (2002).
 [33] J. U. Andersen, E. Bonderup, and K. Hansen, *J. Chem. Phys.* **114**, 6518 (2001).
 [34] J. U. Andersen, E. Bonderup, K. Hansen, P. Hvelplund, B. Lui, U. V. Pedersen, and S. Tomita, *Eur. Phys. J. D* **24**, 191 (2003).
 [35] J. U. Andersen, E. Bonderup, and K. Hansen, *J. Phys. B* **35**, R1 (2002).
 [36] K. Hansen, E. E. B. Campbell, and O. Echt, *Int. J. Mass. Spectrom.* **252**, 79 (2006).
 [37] C. E. Klots, *Z. Phys. D* **20**, 105 (1991).
 [38] B. Tspinyuk, A. Budrevich, M. Grinberg, and E. Kolodney, *J. Chem. Phys.* **106**, 2449 (1997).
 [39] S. Tomita, J. U. Andersen, K. Hansen, and P. Hvelplund, *Chem. Phys. Lett.* **382**, 120 (2003).
 [40] B. Concina, K. Gluch, S. Matt-Leubner, O. Echt, P. Scheier, and T. D. Märk, *Chem. Phys. Lett.* **407**, 464 (2005).
 [41] K. Gluch, S. Matt-Leubner, O. Echt, B. Concina, P. Scheier, and T. D. Märk, *J. Chem. Phys.* **121**, 2137 (2004).
 [42] I. V. Hertel, H. Steger, J. de Vries, B. Weisser, C. Menzel, B. Kamke, and W. Kamke, *Phys. Rev. Lett.* **68**, 784 (1992).
 [43] H. Steger, J. de Vries, B. Kamke, and W. Kamke, *Chem. Phys. Lett.* **194**, 452 (1992).
 [44] R. Wörgötter, B. Dünser, P. Scheier, and T. D. Märk, *J. Chem. Phys.* **101**, 8674 (1994).
 [45] B. Concina, S. Tomita, J. U. Andersen, and P. Hvelplund, *Eur. Phys. J. D* **34**, 191 (2005).
 [46] B. Concina, S. Tomita, N. Takahashi, T. Kodama, S. Suzuki, K. Kikuchi, Y. Achiba, A. Gromov, J. U. Andersen, and P. Hvelplund, *Int. J. Mass. Spectrom.* **252**, 96 (2006).
 [47] S. Matt, O. Echt, P. Scheier, and T. D. Märk, *Chem. Phys. Lett.* **348**, 194 (2001).